3D-Trajectory Design for Outage Minimization in UAV-Assisted 5G Communication System

Nishant Gupta[1], Deepak Mishra[2], and Satyam Agarwal[1]

[1]Department of Electrical Engineering, Indian Institute of Technology Ropar, Punjab, India
[2]School for Electrical Engineering and Telecommunications, University of New South Wales, Sydney, Australia
E-mails: 2018eez0018@iitrpr.ac.in, dph.mishra@gmail.com, satyam6099@gmail.com

2021 IEEE 18th Annual Consumer Communications & Networking Conference (CCNC) | 978-1-7281-9794-4/21/$31.00 ©2021 IEEE | DOI: 10.1109/CCNC49032.2021.9369641

***Abstract*—In this paper, we study and optimize the trajectory for unmanned aerial vehicle (UAV) to provide fifth-generation (5G) cellular service to users in a given area. We consider a single UAV launched from the fixed initial to the final location, during which it serves the ground users that are distributed in a circular field. We introduced an optimization problem to minimize the average outage probability of the system by optimizing the three-dimensional (3D) trajectory of the UAV. As this problem is non-convex, we proposed an efficient approach that involves two steps, firstly it frames a new problem to obtain a globally optimal location in 3D space for minimal average outage probability. This problem is shown to be conditionally convex and an efficient algorithm is proposed to obtain a globally optimal location within an acceptable tolerance. Thereafter, a sub-optimal solution is proposed for the original problem. Simulation results provide useful insights into the sub-optimal trajectory of UAV and show that our proposed approach on an average provides 24% outage improvement over the benchmark scheme. This improvement is further enhanced with the increase in the velocity of UAV.**

***Index Terms*—UAV communication, outage probability, trajectory optimization, 5G communication.**

I. Introduction

The fifth-generation of mobile communication (5G) will support a higher number of applications and users having varied requirements. In some cases, the terrestrial infrastructure is not sufficient to provide the 5G performance due to high traffic or intrinsic limitations. Unmanned aerial vehicle (UAV) is a promising technology that can contribute to such limitations and can extend wireless coverage to support more number of users [1]. A UAV can be swiftly deployed in a given area of interest to provide on-demand services. Further, they can enhance coverage in a given location due to its establishing line of sight (LoS) communication with the users.

Deployment of UAVs for 5G communication pose several challenges. One such challenge is optimal path planning of UAV to minimize outage probability or maximize coverage [2]. This optimal path planning is useful to develop an efficient model such that the key performance metric should be enhanced.

In literature, several works have been done on optimizing the trajectory of a UAV with a focus on maximizing the energy efficiency of the UAV, where it flies over a fixed altitude [3]. Some research have focused on minimizing the outage probability of the relay network by optimizing the UAV trajectory and the transmit power, in an uplink scenario [4].

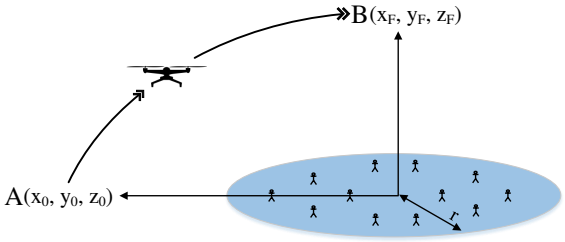

Fig. 1. System model representing the coverage area having N users in 2D plane along with UAV's initial and final locations.

In [5] and [6], the outage probability was minimized for the dual-slope path loss based on the two-ray model. The authors in [7] maximized the minimum data collection rate in a UAV-enabled wireless sensor network. Optimal UAV altitude for outage minimization was derived in the presence of fading to maximize coverage under the probabilistic LoS channel model in [8], and [9]. In [10], the UAV mission completion time was minimized by optimizing its horizontal trajectory while maintaining a minimum signal-to-noise ratio (SNR).

UAV as an aerial base station is highly efficient to support burst crowds in scenarios, such as, festivals, carnivals, musical performances, sports activities, and many more, where a large number of people are expecting better coverage. These advantages have encouraged us to optimize the three-dimensional (3D) trajectory of the UAV while maintaining efficient communication in terms of minimal outage probability. A more practical UAV channel model is to consider LoS and non-LoS (NLoS) occurrence probability in channel link. This takes into account the randomness of building heights [11]. To the best of our knowledge, there is no work carried out on optimizing the 3D trajectory of UAV by minimizing the outage probability of a system where the UAV-ground links are modelled on occurrence probabilities of LoS and NLoS links. Moreover, previous works assume UAV flying at a constant altitude or finds the optimal altitude, which restricts the use of UAVs in practical scenario.

II. System Model

In this work, we consider a wireless communication system, where a UAV is launched from location $\mathrm{A}(\mathrm{x}_0, \mathrm{y}_0, \mathrm{z}_0)$ and

978-1-7281-9794-4/21/$31.00 ©2021 IEEE

moves to a final location $\mathrm{B}(\mathrm{x_F}, \mathrm{y_F}, \mathrm{z_F})$ to provide coverage in a two-dimensional (2D) circular field of radius r. $\mathrm{x}_0, \mathrm{y}_0 \in \mathbb{R}$ and $\mathrm{x_F}, \mathrm{y_F} \in \mathbb{R}$ denote the initial and final horizontal coordinates, respectively, and $\mathrm{z}_0, \mathrm{z_F} \in \mathbb{R}$ are the respective heights, where $\mathbb{R}$ denotes the set of real numbers. There are N ground users indexed by $\mathcal{N} \triangleq \{1, \cdots, N\}$, distributed randomly in the circular field and are assumed to be stationary. Location of the i^{th}-user is given by 3D cartesian coordinate $(\mathcal{U}_i, 0)$, where $\mathcal{U}_i = [x_i, y_i] \in \mathbb{R}^{1\times 2}$, $\forall i \in \mathcal{N}$. z-coordinate of all users is taken as zero considering the users on the ground plane. The total flight time T of the UAV is discretized into M slots of equal length, indexed by $\mathcal{M} = \{1, \cdots, M\}$. The slot duration is given by $\tau = T/M$, which is chosen such that the UAV is assumed to be stationary within each time slot [12]. Thus, the trajectory of the UAV is approximated as $(x[m], y[m], z[m])$, where $x[m]$ and $y[m]$ denote the horizontal coordinates, and $z[m]$ denotes the corresponding height. The distance between the UAV and the i^{th}-user at any time slot m is given by $d_i[m] = \sqrt{(x[m]-x_i)^2 + (y[m]-y_i)^2 + z[m]^2}$. Velocity of the UAV within each time slot is given by

$$v[m] \triangleq \frac{1}{\tau}\|(x[m], y[m], z[m]) - (x[m-1], y[m-1], z[m-1])\|, \tag{1}$$

where $\|b - b'\|$ is the Euclidean norm of vector b and b' with element wise subtraction. In addition, the initial and final slot locations for the UAV are defined as $(x[0], y[0], z[0]) = (\mathrm{x}_0, \mathrm{y}_0, \mathrm{z}_0)$ and $(x[M], y[M], z[M]) = (\mathrm{x_F}, \mathrm{y_F}, \mathrm{z_F})$, respectively.

The UAV at a relatively high altitude is able to develop a LoS connection with the ground users and due to rich scattering it also undergoes small-scale fading [13]. Then, the channel between the UAV and i^{th}-user at the m^{th} time slot is modelled as $g_i[m] = \sqrt{\mathcal{L}_i[m]}\tilde{h}_i[m]$, where $\mathcal{L}_i[m]$ accounts for large-scale fading that is responsible for the attenuation of signal including path loss and shadowing. $\tilde{h}_i[m]$ accounts for small-scale fading and is modelled by Rayleigh fading with $\mathbb{E}[|\tilde{h}_i[m]|^2] = 1$. In addition, large-scale attenuation for UAV-ground links are usually modelled as a random variable based on the occurrence probabilities of LoS and NLoS components [3]. Their path loss expression are given as

$$\mathcal{L}_i[m] = \begin{cases} d_0 d_i[m]^{-\bar{\alpha}}, \text{ for LoS link, and} \\ \kappa d_0 d_i[m]^{-\bar{\alpha}}, \text{ for NLoS link,} \end{cases} \tag{2}$$

where d_0 represents the path loss at a reference distance of 1 meter, $\bar{\alpha}$ represents the path loss exponent, and $\kappa < 1$ accounts for additional attenuation factor due to NLoS component. The probability that the i^{th}-user is in LoS with the UAV at time slot m is represented as a logistic function of elevation angle [9] and is given by

$$P_{LoS} = \frac{1}{1 + C\exp(-D[\phi_i[m] - C])}, \tag{3}$$

where C and D are parameters depending on environment, such as rural, sub-urban and urban. $\phi_i[m]$ (in degrees) is the elevation angle of UAV from i^{th}-user at time slot m given as $\phi_i[m] = \frac{180}{\pi}\sin^{-1}\left(\frac{z[m]}{d_i[m]}\right)$. Channel $g_i[m]$ is a random variable which includes the random occurrence of LoS and NLoS links, and also the random small-scale fading. The expected power gain of channel by averaging over the above randomness is given by [14]

$$\mathbb{E}[|g_i[m]|^2] = P_{LoS} d_0 d_i[m]^{-\bar{\alpha}} + (1 - P_{LoS})\kappa d_0 d_i[m]^{-\bar{\alpha}}. \tag{4}$$

Let P_{tr} represent the transmit power of the UAV. The average SNR, denoted by $\gamma_i[m]$, between the i^{th}-user and the UAV at time slot m is given as $\gamma_i[m] = \frac{P_{tr}|g_i[m]|^2}{\sigma_n^2}$. Substituting (4) in $\gamma_i[m]$, we get [3, Eq. 10]

$$\gamma_i[m] = \frac{\tilde{\gamma}_o((1-\kappa)P_{LoS} + \kappa)}{((x[m]-x_i)^2 + (y[m]-y_i)^2 + z[m]^2)^{\alpha}}, \tag{5}$$

where $\tilde{\gamma}_o \triangleq P_{tr} d_0/\sigma_n^2$, σ_n^2 is the channel noise power and $\alpha \triangleq \bar{\alpha}/2$. Outage probability of the i^{th}-user, defined as the probability that the received SNR falls below the threshold γ_{th} [15] is given as $P_{out}^i[m] = 1 - e^{-\frac{\gamma_{th}}{\gamma_i[m]}}$. Substituting (5) in $P_{out}^i[m]$, the outage probability is given by

$$P_{out}^i[m] = 1 - e^{\left(-\frac{\gamma_{th}}{\tilde{\gamma}_o}\frac{((x[m]-x_i)^2 + (y[m]-y_i)^2 + z[m]^2)^{\alpha}}{(1-\kappa)P_{LoS} + \kappa}\right)}. \tag{6}$$

Next, we formulate an optimization problem to minimize the outage probability defined in (6).

III. Problem Formulation

We intent to minimize the outage probability averaged over time and users under the constraints on UAV trajectory. The optimization problem is formulated as

$$\text{(P1)}: \min_{\substack{\{x[m], y[m], z[m]\} \\ \forall\, m \in \mathcal{M}}} \quad \frac{1}{MN}\sum_{m=1}^{M}\sum_{i=1}^{N} P_{out}^i[m]$$

$$\text{subject to (s.t.)}: (C1): (x[M], y[M], z[M]) = (\mathrm{x_F}, \mathrm{y_F}, \mathrm{z_F}),$$
$$(C2): z[m] \geq H, \forall m \in \mathcal{M} - \{M\},$$
$$(C3): v[m] \leq V_{max}, \forall m \in \mathcal{M},$$

where $(C1)$ represents the final location constraint, and $(C2)-(C3)$ represent the minimum height required by the UAV to avoid collisions and the maximum velocity constraint of the UAV, respectively. To obtain the optimal solution, we first present the following proposition, and then we check the feasibility of (P1).

Proposition 1: Using $\widehat{P}_{out}^i[m]$ defined below instead of $P_{out}^i[m]$ defined in (6) in (P2) is equivalent.

$$\widehat{P}_{out}^i[m] \triangleq \frac{\frac{\gamma_{th}}{\tilde{\gamma}_o}((x[m]-x_i)^2 + (y[m]-y_i)^2 + z[m]^2)^{\alpha}}{\frac{(1-\kappa)}{1 + Ce^{\left(-D\left[\frac{180}{\pi}\sin^{-1}\left(\frac{z[m]}{\sqrt{(x[m]-x_i)^2 + (y[m]-y_i)^2 + z[m]^2}}\right) - C\right]\right)}} + \kappa}. \tag{7}$$

Proof: Using $e^{-a} \approx 1 - a$, $\forall\, a \ll 1$, in (6), since the $P_{out}^i[m]$ is a strictly increasing function of $\widehat{P}_{out}^i[m]$, the two optimization problems with objective functions $\widehat{P}_{out}^i[m]$ and $P_{out}^i[m]$ are equivalent and share the same set of optimal points $(x^*[m], y^*[m], z^*[m])$ [16]. The optimal values are related as $P_{out}^{i*}[m] = 1 - e^{-\widehat{P}_{out}^{i*}[m]}$. ∎

Now according to $(C2)$ in (P1), the vertical coordinate of the optimized trajectory should always be greater than H for all $m \in \mathcal{M} - \{M\}$. The issue lies in the first few and last

few time slots. This is because the problem becomes infeasible when the z-coordinate of $(\mathrm{x}_0, \mathrm{y}_0, \mathrm{z}_0)$ and $(\mathrm{x}_\mathrm{F}, \mathrm{y}_\mathrm{F}, \mathrm{z}_\mathrm{F})$ is lesser than H and the following condition defined below for initial and final locations are not satisfied

$$\mathrm{z}_0 + \tau V_{max} \geq H, \text{ and } \mathrm{z}_\mathrm{F} + \tau V_{max} \geq H. \tag{8}$$

To address this issue, we find the number of slots for which the problem (P1) becomes feasible. We assume that the UAV moves with V_{max} and it does not show any lateral movement until it reaches a certain height that satisfies (8), then, $S_h^I = \lfloor H/\tau V_{max} \rfloor$ is defined as the time slots required to attain that height. Same is applicable for final location and we denote the time slots with S_h^F. Then, $\mathcal{M}_f = \{S_h^I + 1, \cdots, M - S_h^F\}$ which reduces to $\mathcal{M} = \{1, \cdots, M\}$ when $S_h^I = 0$ and $S_h^F = 0$ *i.e.,* when (P1) is feasible beforehand. Then, the new initial and final locations are given as $(\mathrm{x}_0, \mathrm{y}_0, \bar{z}_I \triangleq S_h^I \tau V_{max})$ and $(\mathrm{x}_0, \mathrm{y}_0, \bar{z}_F \triangleq S_h^F \tau V_{max})$, respectively. Then using Proposition 1 and feasibility criteria, (P1) is defined as

$$\text{(P2)}: \min_{\substack{\{x[m], y[m], z[m]\} \\ \forall\, m \in \mathcal{M}_f}} \quad \frac{1}{MN} \sum_{m=1}^{M} \sum_{i=1}^{N} \widehat{P}_{out}^i[m]$$

$$\text{s.t. } (C4): z[m] \geq H, \forall m \in \mathcal{M}_f - \{M - S_h^F\},$$
$$(C5): (x[M - S_h^F], y[M - S_h^F], z[M - S_h^F]) = (\mathrm{x}_\mathrm{F}, \mathrm{y}_\mathrm{F}, \bar{z}_F),$$
$$(C6): v[m] \leq V_{max}, \forall m \in \mathcal{M}_f.$$

Next, we propose the solution methodology to solve (P2).

IV. Proposed Methodology

It is observed that $\widehat{P}_{out}^i[m]$ in expression (7) depends upon $\{x[m], y[m], z[m]\}$,$\forall m \in \mathcal{M}_f$, not only via distance between the UAV and the user but also via probability of LoS, P_{LoS}, which makes problem difficult to handle and we cannot achieve the optimal solution directly. Therefore, we decomposed the original problem (P2) into two points. First, we obtain UAV trajectory by relaxing $(C6)$ in (P2) to get insights on drone trajectory. Thereafter, we solve the original problem (P2) by using the solution to the former problem.

A. UAV Trajectory by Relaxing $(C6)$ in (P2)

Due to no constraint on velocity, the UAV will reach the best location with the minimum average outage probability in a single time slot. Moreover, for any other time slot $m \in \mathcal{M} - \{M\}$, it will stay at that location. As the average outage probability is a function of location of ground users $(x_i, y_i), \forall i \in \mathcal{N}$, and UAV, so we will get a single location of UAV in 3D space where the average outage probability is minimum.

Thus, the optimal trajectory when $(C6)$ is relaxed will consists of only three distinct locations that are, the initial, the optimal, and the final locations, where for all $m = \{1, \cdots, M-1\}$ time slots the UAV will be present at the optimal location. Based on above discussion, we need to find the optimal location where average outage probability is minimum. Therefore, we define a new optimization problem by omitting [m] as:

$$\text{(P3)}: \min_{\{x,y,z\}} \bar{P}_{out} \quad \text{s.t.} \quad -r \leq x, y \leq r, H \leq z \leq H_{max},$$

Algorithm 1 ϵ-globally optimal solution

Input: $-r \leq x \leq r$, $-r \leq y \leq r$, $H \leq z \leq H_{max}$, N, $(x_i, y_i), \forall i \in \mathcal{N}$, $\mathcal{R}$ and ϵ.
Output: $\bar{P}_{out}^*$ with $\mathcal{X}_\epsilon^* = (x^*, y^*, z^*)$.
1: Compute $\mathcal{R}_C^i, \forall i \in \mathcal{N}$, and $\mathcal{R}_C$, using (A.7) and (A.8), respectively, as defined in Appendix A.
2: Let $\mathcal{X}_\epsilon = (x, y, z)$. For $\mathcal{R}_C$, compute $\mathcal{X}_1^* = arg \min_{\mathcal{X}_\epsilon} \bar{P}_{out}$ using GSS with ϵ.
3: Evaluate $\mathcal{X}_2^* = arg \min_{\mathcal{X}_\epsilon} \bar{P}_{out}$ using linear search over the region $\mathcal{R}_{NC} = \mathcal{R}/\mathcal{R}_C$ by keeping step size ϵ.
4: Obtain $\mathcal{X}_\epsilon^* = arg \min_{\{\mathcal{X}_j^*\}} \bar{P}_{out}$ for $j \in \{1, 2\}$.
5: Set $\bar{P}_{out}^*$ to $\bar{P}_{out}$ corresponding to $\mathcal{X}_\epsilon^*$.

where $\bar{P}_{out} \triangleq \frac{1}{N} \sum_{i=1}^{N} \widehat{P}_{out}^i$. Since the users are present in a coverage field of radius r, centered at origin, the optimal values of x and y will always lie within the coverage field, then, $-r \leq x, y \leq r$. H_{max} is chosen such that the outage probability of field edge user is approximately one when UAV hovers over the centre of the field.

In (P3), since $\bar{P}_{out}$ is non-convex in x, y, and z, it is difficult to obtain the globally optimal solution. Thus, in our proposed solution we ensure that our result remains in the ϵ-neighbourhood of globally optimal solution. We term our proposed solution as ϵ-globally optimal solution, where ϵ is defined as the acceptable tolerance. To find this, we first prove the conditional convexity of $\bar{P}_{out}$. Then, by using it, we reduce the overall complexity of the solution by applying golden section search (GSS) in the convex region [17], and linear search in the non-convex region. Next, we find the region of joint convexity of $\bar{P}_{out}$ in x, y, and z.

Lemma 1: The region over which $\bar{P}_{out}$ is jointly convex in x, y, and z is given by $\mathcal{R}_C$, where $\mathcal{R}_C$ is defined by (A.8).

Proof: See Appendix A. ∎

The problem (P3) is convex in region $\mathcal{R}_C$ and non-convex in the region $\mathcal{R}_{NC} = \mathcal{R}/\mathcal{R}_C$, where $\mathcal{R}$ is the region defined by $-r \leq x \leq r$, $-r \leq y \leq r$, and $H \leq z \leq H_{max}$. Then first, by applying GSS in $\mathcal{R}_C$ with acceptable tolerance ϵ and later using linear search in $\mathcal{R}_{NC}$ by taking the step size ϵ, we can obtain two sub-optimal solutions within an acceptable tolerance ϵ. One of the solutions is set to a globally optimal solution for which the $\bar{P}_{out}$ is minimum, and the solution obtained is termed as the ϵ-globally optimal solution. Algorithm 1 describes the steps to obtain the ϵ-globally optimal solution $\mathcal{X}_\epsilon^*$ for (P3).

Then, the path traced by the UAV in travelling from the initial to $\mathcal{X}_\epsilon^*$ and then to the final location while hovering at $\mathcal{X}_\epsilon^*$ for all $m \in \mathcal{M} - \{M\}$ is defined as the optimal path of (P2) when $(C6)$ is relaxed. The optimal velocity V_{opt} is obtained in which distance travelled by UAV is maximum *i.e,* $V_{opt} = \max\left\{\frac{\|(\mathrm{x}_\mathrm{F}, \mathrm{y}_\mathrm{F}, \bar{z}_F) - \mathcal{X}_\epsilon^*\|}{\tau}, \frac{\|(\mathrm{x}_0, \mathrm{y}_0, \bar{z}_I) - \mathcal{X}_\epsilon^*\|}{\tau}\right\}$. The presence of $(C6)$ will restrict the UAV in reaching the $\mathcal{X}_\epsilon^*$ in a single time slot. Thus in the next sub-section, we will find the UAV trajectory while considering the velocity constraint $(C6)$.

B. Proposed Trajectory for (P2)

Since we have obtained the ϵ-globally optimal solution $\mathcal{X}_\epsilon^*$ from (P3), where the average outage probability is minimum in

Algorithm 2 Proposed solution of (P2)

Input: $(\mathrm{x}_0, \mathrm{y}_0, \bar{z}_I)$, $(\mathrm{x}_F, \mathrm{y}_F, \bar{z}_F)$, S_h^I, S_h^F, M, $\mathcal{M}_f$, N, V_{max}, $(x_i, y_i), \forall i \in \mathcal{N}$, τ, and ϵ.

Output: $\widehat{P}^*_{avg}$ with $(x^*[m], y^*[m], z^*[m]), \forall m \in \mathcal{M}_f$.

1: Find optimal location $\mathcal{X}^*_\epsilon$ using Algorithm 1.
2: Calculate $d_1 = \|(\mathrm{x}_0, \mathrm{y}_0, \bar{z}_I) - \mathcal{X}^*_\epsilon\|$, $d_2 = \|\mathcal{X}^*_\epsilon - (\mathrm{x}_F, \mathrm{y}_F, \bar{z}_F)\|$ and $M_1 = \left\lceil \frac{d_1}{\tau V_{max}} \right\rceil$, $M_2 = \left\lceil \frac{d_2}{\tau V_{max}} \right\rceil$.
3: **if** $M_1 + M_2 \leq M - S_h^F$ **then**
4: Make a straight line from $(\mathrm{x}_0, \mathrm{y}_0, \bar{z}_I)$ to $\mathcal{X}^*_\epsilon$ and from $\mathcal{X}^*_\epsilon$ to $(\mathrm{x}_F, \mathrm{y}_F, \bar{z}_F)$ each containing M_1 and M_2 locations, respectively. For $M - S_h^F - (M_1 + M_2)$ time slots, the UAV will stay at $\mathcal{X}^*_\epsilon$.
5: Set the obtained locations as solution *i.e.,* $(x^*[m], y^*[m], z^*[m])$, $\forall m \in \mathcal{M}_f$, and obtain $\widehat{P}^*_{avg} \triangleq \frac{1}{(M - S_h^F - S_h^I)N} \sum_{m=S_h^I+1}^{M-S_h^F} \sum_{i=1}^{N} \widehat{P}^i_{out}[m]$ by calculating $\widehat{P}^i_{out}[m]$ using (7).
6: **else**
7: Calculate $d_{exp} = \tau(M - S_h^I - S_h^F)V_{max}$.
8: Find $(\mathrm{x}_{\epsilon 2}, \mathrm{y}_{\epsilon 2}, \mathrm{z}_{\epsilon 2})$ that satisfies $\|(\mathrm{x}_0, \mathrm{y}_0, \bar{z}_I) - (\mathrm{x}_{\epsilon 2}, \mathrm{y}_{\epsilon 2}, \mathrm{z}_{\epsilon 2})\| + \|(\mathrm{x}_{\epsilon 2}, \mathrm{y}_{\epsilon 2}, \mathrm{z}_{\epsilon 2}) - (\mathrm{x}_F, \mathrm{y}_F, \bar{z}_F)\| = d_{exp}$, where $(\mathrm{x}_{\epsilon 2}, \mathrm{y}_{\epsilon 2}, \mathrm{z}_{\epsilon 2})$ belongs to line segment joining $\mathcal{X}^*_\epsilon$ and mid-point of straight flight trajectory.
9: Repeat step 2 and step 4 with $(\mathrm{x}_{\epsilon 2}, \mathrm{y}_{\epsilon 2}, \mathrm{z}_{\epsilon 2})$ instead of $\mathcal{X}^*_\epsilon$ to obtain trajectory and calculate $\widehat{P}^*_{avg}$ using step 5.

comparison with any other location. Thus, our objective here is to reach the $\mathcal{X}^*_\epsilon$ as quickly as possible and stay there for longer periods of time. In case, due to insufficient velocity, if the UAV cannot reach the $\mathcal{X}^*_\epsilon$, then it should at least approach that location while travelling towards the final location. This implies, the UAV will move with V_{max} in this approach.

Whenever $V_{max} \geq V_{opt}$ in $(C6)$, the velocity constraint will not affect the trajectory. This is because the UAV can still reach $\mathcal{X}^*_\epsilon$ in a single time slot. Then, V_{opt} can be treated as upper bound on the velocity. However, if $V_{max} < V_{opt}$, the UAV will first move towards the direction of $\mathcal{X}^*_\epsilon$ and then towards the final location. This implies the UAV now takes $m \in \mathcal{M}_f$ number of time slots to reach $\mathcal{X}^*_\epsilon$. As a result, the sub-optimal path consists of many locations while travelling towards $\mathcal{X}^*_\epsilon$ and then towards final location, where for every other location the average outage probability will be higher than $\mathcal{X}^*_\epsilon$. Therefore, $\widehat{P}_{avg}$ will always be higher than that obtained for (P2) when $(C6)$ is relaxed. Thus, the $\widehat{P}_{avg}$ obtained while relaxing $(C6)$ in (P2) is defined as lower bound on $\widehat{P}_{avg}$ for (P2). The steps to obtain the solution of (P2) is described in Algorithm 2. Next, we discuss the performance analysis of the proposed approach and compare it with benchmark scheme.

V. Results and Discussion

In this section, we present the 3D UAV trajectory, and its performance for the proposed approach is shown and compared with the benchmark scheme. We consider a setup with 10 users [18], randomly distributed in a circle of radius 130 m, centered at the origin. The UAV is assumed to fly from the initial location $(-150, 0, 0)$ m towards $(0, 0, 150)$ m. The default parameters taken for simulations are reference SNR $\tilde{\gamma}_o = 52.5$ dB, threshold SNR $\gamma_{th} = -3.01$ dB, and $\epsilon = 1 \times 10^{-6}$. Modelling parameters for LoS channel are taken as $C = 10$, $D = 0.6$, $\kappa = 0.2$, and path loss exponent $\bar{\alpha} = 2.3$ [3].

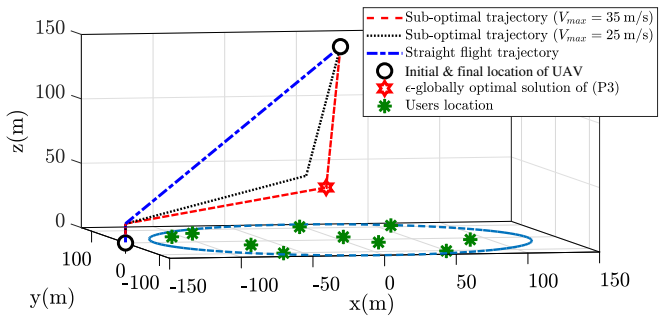

Fig. 2. Sub-optimal trajectory of UAV with $V_{max} = \{35, 25\}$ m/s.

Through Fig. 2, we provide insights into the 3D UAV trajectory. It is plotted with different V_{max} by assuming $T = 20$ s, $M = 50$, and $H = 15$ m. Along with the sub-optimal trajectories, the ϵ-globally optimal solution $\mathcal{X}^*_\epsilon$ of (P3), and the user's location is also shown. It can be seen in figure, for $V_{max} = 35$ m/s, the UAV will first fly towards $\mathcal{X}^*_\epsilon$ and then travels to the final location in a straight line with velocity V_{max} while hovering at the $\mathcal{X}^*_\epsilon$. But for $V_{max} = 25$ m/s, due to lesser velocity, it cannot reach $\mathcal{X}^*_\epsilon$. Thus, it tries to approach $\mathcal{X}^*_\epsilon$ while travelling towards the final location. Also, it can be seen that the UAV first shows only vertical movement, to satisfy $(C2)$ as defined in Section III.

Next, to understand how the location of UAV is changing with the time slot, we plot Fig. 3. Figs. 3(a)-(c) show the variation of x^*, y^*, and z^* for different values of H in $(C4)$ and V_{max} in $(C6)$, where for H in $(C4)$, V_{max} is set to 30 m/s and for V_{max} in $(C6)$, H is set to 15 m. Other parameters T, and M are set to 20 s, and 50. Since the solution of (P2) is dependent on H, the higher value of H corresponds to more number of time slots required by the UAV to satisfy H and then to reach $\mathcal{X}^*_\epsilon$. It can be observed that the UAV will first fly vertically upwards by keeping the x and y coordinate constant and after that, it will fly towards $\mathcal{X}^*_\epsilon$. As a result, the time spent at that location decreases. Furthermore, as V_{max} decreases, the time spent at $\mathcal{X}^*_\epsilon$ decreases and with a very less V_{max}, the UAV will never reach that location, instead reaches to a certain midway point while following the above location and then fly to its final location as shown in Fig. 3. The horizontal overlapped part in the sub-plots of Figs. 3(a)-(c) show the comparison of slots for which the UAV is present at ϵ-globally optimal solution $\mathcal{X}^*_\epsilon$.

As in Fig. 2, we have seen that when we decreased the velocity, the sub-optimal path moves away from $\mathcal{X}^*_\epsilon$. Then, to understand the impact of $\widehat{P}_{avg}$ with V_{max} and flight time T, we plot Figs. 4, and 5. Fig. 4 is plotted against V_{max} for different $T = \{100, 120, 140\}$ s. Fig. 5 is plotted against T for three different values of $V_{max} = \{20, 25, 30\}$ m/s. In the proposed approach, the UAV moves with V_{max} to reach $\mathcal{X}^*_\epsilon$ and then to final location, increasing V_{max} and T will allow it to reach that location in less time. Consequently, it will spend more time at that location before travelling towards the final location. This will achieve better $\widehat{P}_{avg}$, and since $\mathcal{X}^*_\epsilon$ corresponds to minimum average outage probability, spending

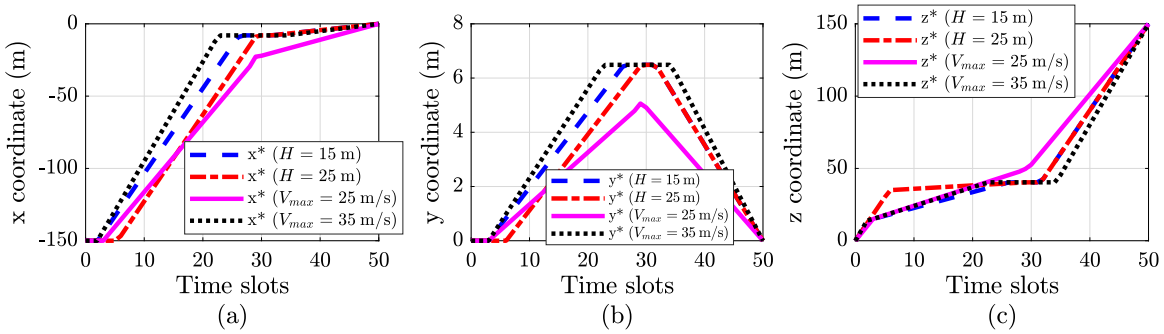

Fig. 3. Variation of (a) x^*, (b) y^*, and (c) z^* with number of time slots for different values of H and V_{max} in constraint $(C4)$ and $(C6)$, respectively.

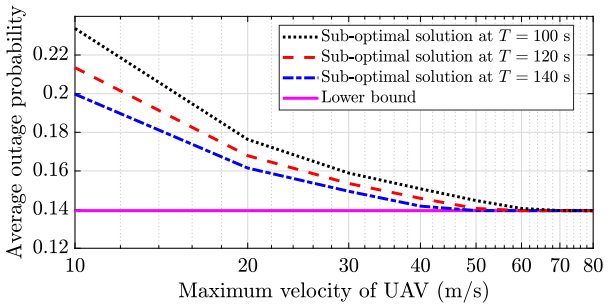

Fig. 4. Variation of average outage probability with V_{max} at different T.

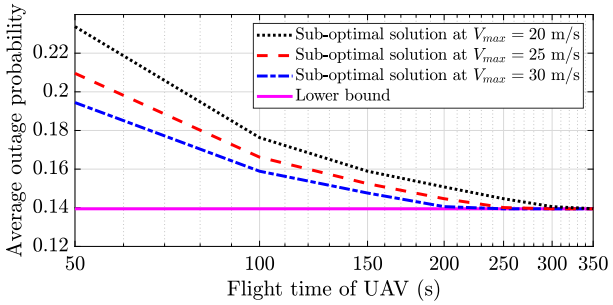

Fig. 5. Variation of average outage probability with T at different V_{max}.

more and more time at that location will decrease it, and it will finally converge to the lower bound of $\widehat{P}_{avg}$ for (P2).

Finally, we present the $\widehat{P}_{avg}$ performance enhancement results achieved with the proposed approach over the benchmark (straight flight trajectory) in Fig. 6. On one hand, results plotted in Fig. 6 shows that improvement in $\widehat{P}_{avg}$ (in %) increases with T for fixed V_{max}. On the other hand, improvements in $\widehat{P}_{avg}$ (in %) may decrease or increase with an increase in H. This happens because with an increase in H, the chances for LoS links may increase but on the contrary increasing the height will also decrease the channel gain. Finding the optimal height at which the outage probability obtained is minimum is out of the scope of this paper. In fact, for both the cases as V_{max} increases from 25 m/s to 35 m/s, the percentage improvement in $\widehat{P}_{avg}$ also increases (30% to up to 38% for fixed $T = 40$ s).

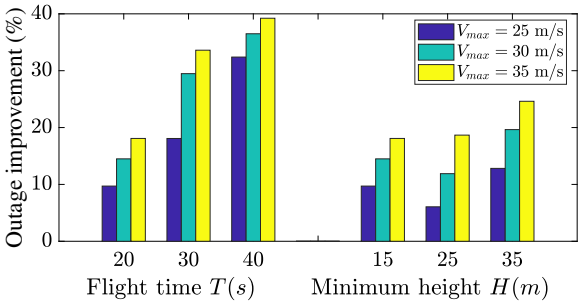

Fig. 6. Percentage outage probability with respect to straight flight trajectory.

VI. Conclusion

We proposed the 3D trajectory design for a UAV-assisted 5G communication system to minimize the average outage probability over all time. To solve this, we present an efficient approach that depends upon the globally optimal location within an acceptable tolerance and constructs trajectory based on that location. The globally optimal location is the location where the UAV should be deployed to attain minimum average outage probability. The conditional joint convexity of the outage probability is proved to obtain the globally optimal location within an acceptable tolerance. Extensive simulations show that the proposed approach shows better average outage probability compared to the benchmark scheme. Besides, the globally optimal location obtained in this approach could be used as a referential baseline to obtain the lower bound on average outage probability.

Appendix A
Conditional Joint Convexity of $\bar{P}_{out}$ in x, y, and z

Although $\bar{P}_{out}$ is non-convex with respect to x, y, and z, we can still find the region where $\bar{P}_{out}$ is jointly convex. Since $\bar{P}_{out} = \frac{1}{N}\sum_{i=1}^{N} \widehat{P}^i_{out}$, we will first find the condition of joint convexity for $\widehat{P}^i_{out}$ in x, y, and z, then, we will show the region in which $\bar{P}_{out}$ is jointly convex.

For ease of proving the joint conditional convexity of $\widehat{P}^i_{out}$ in x, y, and z, we consider the following substitution in (7) as $L_i \triangleq \sqrt{(x-x_i)^2 + (y-y_i)^2}, i \in \mathcal{N}$, where L_i represents the horizontal distance between the projection of UAV on the ground and the i^{th}-user. L_i can also be written in form of $L_i = \sqrt{f(x,y)}$, where $f(x,y) = (x-x_i)^2 + (y-y_i)^2$. The function $f(x,y)$ has $\frac{\partial^2 f(x,y)}{\partial x^2} = 2$, $\frac{\partial^2 f(x,y)}{\partial y^2} = 2$, and $\frac{\partial^2 f(x,y)}{\partial y \partial x} = \frac{\partial^2 f(x,y)}{\partial x \partial y} = 0$, then, $det[\mathcal{H}(f(x,y))] > 0$, where $\mathcal{H}(f(x,y)) = \begin{bmatrix} \frac{\partial^2 f(x,y)}{\partial x^2} & \frac{\partial^2 f(x,y)}{\partial x \partial y} \\ \frac{\partial^2 f(x,y)}{\partial y \partial x} & \frac{\partial^2 f(x,y)}{\partial y^2} \end{bmatrix}$, this implies $f(x,y)$ is a jointly convex in x, and y. Since square root is a monotonic

increasing function, therefore it preserves the convexity [19]. This implies L_i is jointly convex in x, and y. Then, $\widehat{P}^i_{out}$ obtained by substituting L_i in (7) is given as:

$$\widehat{P}^i_{out} \triangleq \frac{\frac{\gamma_{th}}{\tilde{\gamma}_o}(L_i^2+z^2)^{\alpha}}{\frac{(1-\kappa)}{1+C\exp\left(-D\left[\frac{180}{\pi}\sin^{-1}\left(\frac{z}{\sqrt{L_i^2+z^2}}\right)-C\right]\right)}+\kappa}. \quad (A.1)$$

Now, if we prove that $\widehat{P}^i_{out}$ is a conditional jointly convex in L_i, and z, the same can be applied to x, y, and z. In order to prove the conditional convexity, we considered a single user. Then, the Hessian matrix of $\widehat{P}^i_{out}$ defined in (A.1) is given by $\mathcal{H}(\widehat{P}^i_{out}) = \begin{bmatrix} \frac{\partial^2 \widehat{P}^i_{out}}{\partial L_i^2} & \frac{\partial^2 \widehat{P}^i_{out}}{\partial L_i \partial z} \\ \frac{\partial^2 \widehat{P}^i_{out}}{\partial z \partial L_i} & \frac{\partial^2 \widehat{P}^i_{out}}{\partial z^2} \end{bmatrix}$, where

$$\frac{\partial^2 \widehat{P}^i_{out}}{\partial L_i^2} = \mathcal{A}_1\Bigg[\frac{180 w_i D z(1-\kappa)}{\pi(w_i\kappa+1)^2}\Bigg(\frac{90 D z(1-w_i\kappa)}{\pi(w_i\kappa+1)} + (2\alpha-1)L_i\Bigg) + \frac{\alpha(w_i+1)\Big((2\alpha-1)L_i^2+z^2\Big)}{w_i\kappa+1}\Bigg], \quad (A.2)$$

$$\frac{\partial^2 \widehat{P}^i_{out}}{\partial z \partial L_i} = \frac{\partial^2 \widehat{P}^i_{out}}{\partial L_i \partial z} = 2\mathcal{A}_1\Bigg[\frac{(\alpha-1)\alpha L_i z(w_i+1)}{w_i\kappa+1} + \frac{45 w_i D(1-\kappa)}{\pi(w_i\kappa+1)^2}\Bigg(\frac{180 D L_i z(w_i\kappa-1)}{\pi(w_i\kappa+1)} - (2\alpha-1)(L_i^2-z^2)\Bigg)\Bigg], \quad (A.3)$$

$$\frac{\partial^2 \widehat{P}^i_{out}}{\partial z^2} = \mathcal{A}_1\Bigg[\frac{180 w_i D L_i(1-\kappa)}{\pi(w_i\kappa+1)^2}\Bigg(\frac{90 D L_i(1-w_i\kappa)}{\pi(w_i\kappa+1)} + (2\alpha+1)z\Bigg) + \frac{\alpha(w_i+1)\Big((2\alpha-1)z^2+L_i^2\Big)}{w_i\kappa+1}\Bigg], \quad (A.4)$$

where $\mathcal{A}_1 = 2\frac{\gamma_{th}}{\tilde{\gamma}_o}\big(L_i^2+z^2\big)^{\alpha-2}$ and $w_i = C\exp\Big(-D\Big(\frac{180}{\pi}\sin^{-1}\Big(\frac{z}{\sqrt{L_i^2+z^2}}\Big)-C\Big)\Big)$. It can be seen that (A.2), $\frac{\partial^2 \widehat{P}^i_{out}}{\partial L_i^2} > 0, \quad \forall L_i, z$ and (A.4), $\frac{\partial^2 \widehat{P}^i_{out}}{\partial z^2} > 0, \quad \forall L_i$, and $z > L_i/4.5$. To show $det[\mathcal{H}(\widehat{P}^i_{out})] > 0$, we need to show that $\mathcal{K}_1 \triangleq \frac{\partial^2 \widehat{P}^i_{out}}{\partial L_i^2} - \frac{\partial^2 \widehat{P}^i_{out}}{\partial z \partial L_i} > 0$, and $\mathcal{K}_2 \triangleq \frac{\partial^2 \widehat{P}^i_{out}}{\partial z^2} - \frac{\partial^2 \widehat{P}^i_{out}}{\partial z \partial L_i} > 0$. Then, if we substitute any value for $z > L_i/4.5$, say $z = L_i/4$ in $\mathcal{K}_1$ and $\mathcal{K}_2$, we get,

$$\mathcal{K}_1 = \mathcal{A}_2\Bigg(2070\pi(2\alpha-1)w_i D(1-\kappa)(w_i\kappa+1) + (w_i+1)\alpha(24\alpha-7)(\pi w_i\kappa+\pi)^2 + 81000 w_i D^2(1-\kappa)(1-w_i\kappa)\Bigg), \quad (A.5)$$

$$\mathcal{K}_2 = \mathcal{A}_2\Bigg(90\pi(46\alpha-7)w_i D(1-\kappa)(w_i\kappa+1) + \alpha(23-6\alpha)(w_i+1)(\pi w_i\kappa+\pi)^2 + 324000 w_i D^2(1-k)(1-w_i\kappa)\Bigg), \quad (A.6)$$

where $\mathcal{A}_2 = \frac{2^{5-4\alpha}17^{\alpha-2}\frac{\gamma_{th}}{\tilde{\gamma}_o}\left(L_i^2\right)^{\alpha-1}}{\pi^2(w_i\kappa+1)^3}$. It can be easily observed that $\mathcal{K}_1 > 0$, and $\mathcal{K}_2 > 0$ from (A.5) and (A.6), respectively. This alongwith (A.2) and (A.4) proves that $\widehat{P}^i_{out}$ is jointly convex in L_i, and z with condition $z > L_i/4.5$. The above condition can be written as

$$\mathcal{R}^i_C \triangleq z^i > \frac{\sqrt{(x-x_i)^2+(y-y_i)^2}}{4.5}. \quad (A.7)$$

The region $\mathcal{R}^i_C$ above represents an inverted cone with center at (x_i, y_i). For each users we obtain similar cones. So, overall the region over which the function is convex is given as the intersection region of all these cones as

$$\mathcal{R}_C = \bigcap_{i=1}^{N} \mathcal{R}^i_C. \quad (A.8)$$

Hence, $\bar{P}_{out}$ is jointly convex in region $\mathcal{R}_C$.

REFERENCES

[1] M. Mozaffari, W. Saad, M. Bennis, Y. Nam, and M. Debbah, "A tutorial on UAVs for wireless networks: Applications, challenges, and open problems," *IEEE Commun. Surveys & Tutorials*, vol. 21, no. 3, pp. 2334–2360, Mar. 2019.

[2] Y. Zeng, R. Zhang, and T. J. Lim, "Wireless communications with unmanned aerial vehicles: opportunities and challenges," *IEEE Commun. Mag.*, vol. 54, no. 5, pp. 36–42, May 2016.

[3] Y. Zeng, J. Xu, and R. Zhang, "Energy minimization for wireless communication with rotary-wing UAV," *IEEE Trans. Wireless Commun.*, vol. 18, no. 4, pp. 2329–2345, Apr. 2019.

[4] S. Zhang, H. Zhang, Q. He, K. Bian, and L. Song, "Joint trajectory and power optimization for UAV relay networks," *IEEE Commun. Lett.*, vol. 22, no. 1, pp. 161–164, Jan. 2018.

[5] S. Zeng, H. Zhang, K. Bian, and L. Song, "UAV relaying: Power allocation and trajectory optimization using decode-and-forward protocol," in *Proc. IEEE ICC Workshops*, Kansas City, USA, May 2018, pp. 1–6.

[6] W. Chen, S. Zhao, and Q. Shi, "Improve stability in UAV relay networks by jointly optimizing communication, trajectory and power," in *Proc. IEEE ICCS*, Chengdu, China, Dec. 2018, pp. 180–185.

[7] C. You, X. Peng, and R. Zhang, "3D trajectory design for UAV-enabled data harvesting in probabilistic LoS channel," in *Proc. IEEE GLOBECOM*, Puako, Hawaii, USA, Dec. 2019, pp. 1–6.

[8] M. M. Azari, F. Rosas, K. Chen, and S. Pollin, "Optimal UAV positioning for terrestrial-aerial communication in presence of fading," in *Proc. IEEE GLOBECOM*, Washington, DC, USA, Dec. 2016, pp. 1–7.

[9] A. Al-Hourani, S. Kandeepan, and S. Lardner, "Optimal LAP altitude for maximum coverage," *IEEE Wireless Commun. Lett.*, vol. 3, no. 6, pp. 569–572, Dec. 2014.

[10] S. Zhang, Y. Zeng, and R. Zhang, "Cellular-enabled UAV communication: A connectivity-constrained trajectory optimization perspective," *IEEE Trans. Commun.*, vol. 67, no. 3, pp. 2580–2604, Mar. 2019.

[11] Y. Zeng, Q. Wu, and R. Zhang, "Accessing from the sky: A tutorial on UAV communications for 5G and beyond," *Proc. IEEE*, vol. 107, no. 12, pp. 2327–2375, 2019.

[12] C. You and R. Zhang, "3D trajectory optimization in rician fading for UAV-enabled data harvesting," *IEEE Trans. Wireless Commun.*, vol. 18, no. 6, pp. 3192–3207, June 2019.

[13] W. Khawaja, I. Guvenc, D. W. Matolak, U. Fiebig, and N. Schneckenburger, "A survey of air-to-ground propagation channel modeling for unmanned aerial vehicles," *IEEE Commun. Surveys & Tutorials*, vol. 21, no. 3, pp. 2361–2391, 2019.

[14] H. Zhao, H. Wang, W. Wu, and J. Wei, "Deployment algorithms for UAV airborne networks toward on-demand coverage," *IEEE J. Sel. Areas Commun.*, vol. 36, no. 9, pp. 2015–2031, Sep. 2018.

[15] A. Goldsmith, *Wireless communications*. Cambridge university press, 2005.

[16] D. Mishra, S. De, and C. Chiasserini, "Joint optimization schemes for cooperative wireless information and power transfer over rician channels," *IEEE Trans. Commun.*, vol. 64, no. 2, pp. 554–571, Feb. 2016.

[17] Y. Chang, "N-dimension golden section search: Its variants and limitations," in *Proc. BMEI*, Tianjin, China, Oct 2009, pp. 1–6.

[18] A. Alsharoa, H. Ghazzai, M. Yuksel, A. Kadri, and A. E. Kamal, "Trajectory optimization for multiple UAVs acting as wireless relays," in *IEEE ICC Workshops*, Kansas City, USA, May 2018, pp. 1–6.

[19] S. Boyd and L. Vandenberghe, *Convex optimization*. Cambridge university press, 2004.